


Design of silica nanoparticle tracers with optimized dispersion stability, sorption and deposition properties based on (X)DLVO and filtration theory

Laura Spitzmüller^{a,b,c,*} , Jonathan Berson^{b,c}, Thomas Kohl^a, Thomas Schimmel^{b,c}, Fabian Nitschke^a

^a Geothermal Energy & Reservoir Technology, Institute of Applied Geosciences, Karlsruhe Institute of Technology, Adenauerring 20b, 76131 Karlsruhe, Germany

^b Institute of Nanotechnology, Karlsruhe Institute of Technology, Hermann-von-Helmholtz-Platz 1, 76344 Eggenstein-Leopoldshafen, Germany

^c Institute of Applied Physics, Karlsruhe Institute of Technology, Wolfgang-Gaede-Straße 1, 76131 Karlsruhe, Germany

ARTICLE INFO

Keywords:

DLVO
Nanoparticle tracer
Silica nanoparticles
XDLVO
Filtration theory
Colloids

ABSTRACT

Functional nanoparticles emerged as potential new tracers for geoscientific applications, such as geothermal reservoir exploration. In this study, optimization strategies based on DLVO, extended DLVO (XDLVO) and filtration theory are presented. Our results show that nanoparticle material should have a low Hamaker constant, making metallic nanoparticles unfavorable. To ensure dispersion stability and minimize sorption on commonly negatively charged reservoir minerals, the nanoparticles should exhibit ζ -potentials below -30 mV. Decreasing the size of nanoparticles increases the diffusion-driven collisions with minerals grains and the probability of deposition while keeping the particle-to-grain size ratio below 0.008 prevents size exclusion effects. The impact of gravity on particle deposition is negligible for nanoparticles, making higher-density nanoparticle tracers viable. Experimental findings and XDLVO theory confirm the applicability of surface modifications to form a steric barrier that lowers attachment efficiencies while increasing colloidal dispersion stability. The impact of temperature cannot be assessed in a straightforward manner as it depends on multiple factors that can have contradicting effects. The presented study can serve as a guideline for the design of stable nanoparticle tracers with predictable transport properties in reservoirs. It shows that selecting appropriate materials, adapting ζ -potentials or employing effective surface modifications are key strategies to improve the performance of engineered nanoparticle tracers for geothermal exploration.

1. Introduction

In recent years, efforts to combine nanotechnology with geoscience emerged. Engineered silica nanoparticles currently find applications as nanofluids in enhanced oil recovery aiming to stabilize emulsions, decrease the interfacial tension, alter rock wettability, increase sweep efficiency and assist in re-mobilizing oil (Chakraborty and Panigrahi, 2020; Gazem et al., 2024; Muneer et al., 2020). Further, the feasibility of functionalization of silica-based nanoparticles offers the possibility of applications as tracer also in challenging environments due to encapsulation of identifiable entities, such as DNA (Alaskar et al., 2015; Chakraborty et al., 2023; Paunescu et al., 2013) or fluorescent molecules (Berson et al., 2024; Rudolph et al., 2020). The encapsulation process has two significant advantages. First, the shielding/protection of the encapsulated identification entity and second, unlike molecules, nanoparticles offer the possibility of surface modifications. Furthermore, this

novel kind of tracers enables tracer multiplicity: using uniquely identifiable tracers with identical transport and sorption properties that allow simultaneous multiple tracer tests, offering insights into geological structures and enabling injections at different points (Spitzmüller et al., 2024b). Field applications of silica-based nanoparticle tracers were reported by Kong et al. (2018) and Mikutis et al. (2018) in shallow groundwater aquifers. Kittilä et al. (2019) tested the applicability of these nanoparticle tracers in the underground laboratory Grimsel, Switzerland and Fan et al. (2024) recorded the successful tracer test using DNA-labeled silica nanoparticles in a strongly acidic (pH 2) geothermal reservoir site in Taiwan, conditions which are known to slow down dissolution (Spitzmüller et al., 2023b). For widespread applications in geological and geothermal reservoirs (elevated temperatures, wide pH ranges), however, stabilizing measures must be taken to increase the stability and ensure the integrity of silica-based nanoparticle tracers (Spitzmüller et al., 2024a). Further open questions regarding

* Corresponding author.

E-mail address: laura.spitzmueller@kit.edu (L. Spitzmüller).

<https://doi.org/10.1016/j.geothermics.2025.103309>

Received 4 November 2024; Received in revised form 11 February 2025; Accepted 5 March 2025

Available online 13 March 2025

0375-6505/© 2025 The Authors. Published by Elsevier Ltd. This is an open access article under the CC BY license (<http://creativecommons.org/licenses/by/4.0/>).

applicability and transportability remain. In the study, theoretical, analytical calculations based on (X)DLVO and filtration theory are made to assess the dispersion stability, sorption tendency and deposition properties to elucidate the requisites for designing silica-based nanoparticle tracers with optimized behavior, such as low sorption affinity and high dispersion stability. This study aims to provide fundamental insight into how to use established colloid science based methods, such as the (X)DLVO theory paired with the filtration theory, which describes the behavior of colloids in (natural) porous media on the pore-scale to design and optimize nanoparticle tracers for geoscience applications, i.e. to elucidate the crucial factors for successful applications.

The classical DLVO theory is used to describe the stability of colloidal dispersion and was developed by Derjaguin and Landau (1941) and Verwey and Overbeek (1948). It sums up the contribution of the attractive London-van der Waals dispersion force and the force originating from the formation of an electric double layer on charged particle surfaces and allows to determine dispersion stability (Adamczyk and Weron, 1999; van Oss, 2008). Accurate knowledge about colloidal dispersion stability, sorption tendency and assessment of risk of aggregation and particle deposition is crucial in many geoscientific applications, such as enhanced oil recovery using nanofluid (Chakraborty and Panigrahi, 2020), environmental remediation processes (Klaine et al., 2009) and tracer tests (Tang et al., 2023). Evaluating the dispersion stability and sorption tendency toward reservoir minerals using DLVO theory is pivotal when aiming to transfer nanoscientific applications to geoscientific research questions (Jia et al., 2024).

Similar to molecular tracers conventionally used in geothermal science and hydrology to assess reservoir conditions and properties, such as extension and interconnection, particle tracer transport properties are determined by advection, diffusion, dispersion and sorption (Bradford et al., 2002). Therefore, in addition to dispersion stability, the impact of fluid dynamics on the transport properties and deposition of nanomaterials in geoscientific environments needs to be considered (Higgo et al., 1993; Liu et al., 2019; Ryan and Elimelech, 1996). Tufenkji and Elimelech (2004) developed a novel solution for the convective-diffusion equation of the classical filtration theory that also considers nanoparticle-related factors, such as hydrodynamic interactions and van der Waals attraction. The equation consists of three parts: the contributions to the filtration process by diffusion, interception and gravity. Together, they represent the single grain collector contact efficiency, i.e., they give an overview of the probability of collision of a transported particle with the reservoir medium (treated as individual single grains in Elimelech et al. (1995)). Pairing this theoretical value with measured or calculated attachment efficiencies, i.e., if sorption is reversible or irreversible, the single grain collector removal efficiency is determined. This value describes the overall tendency of particles to deposit within and be filtered by porous media (Elimelech et al., 1995).

Ideal nanoparticle tracer particles should exhibit minimal sorption and retention and a high dispersion stability, i.e., the repulsive forces in DLVO theory should exceed the attractive ones. However, these forces are partly dependent on extrinsic parameters, such as the salinity of fluids that cannot be adapted. Therefore, for the development of nanotracers, the focus should lay on the surface of the nanoparticles themselves. Here, the advantage of nanoparticles comes into focus: Their modularity enables modification of the surface. By modifying the surface properties of the particles, the ζ -potential can be altered and additional forces are created, such as steric force originating from surfactants/ligands/polymers bound to the surface. The impact of steric force is described by the extended DLVO (XDLVO) theory. Surfactants, such as for example the anionic sodium dodecyl sulfate (SDS) or the zwitterionic SB3-14, additionally increase the dispersion stability (Zareei et al., 2018) and polymer-coated nanoparticles proved to be less sorptive and more stable in high saline fluids compared to unmodified ones (Li et al., 2014). However, if the surfactant concentration is above the critical micelle concentration (CMC), the effect of steric stabilization

could also be reversed due to depletion effects and free micelles, resulting in destabilization of the dispersion (Jódar-Reyes et al., 2006). Therefore, design calculations should also account for the importance of XDLVO theory.

As shown in Spitzmüller et al. (2024b), applying silica nanoparticle-based tracers as (hydro)geological tracers aims to augment the toolbox of available tracer candidates for geothermal and hydrogeological tracer tests. Therefore, the sorption tendency of these nanoparticle tracers and their deposition in reservoir media needs to be assessed and the governing deposition mechanisms elucidated (Liu et al., 2019). Additionally, to facilitate the design of suitable nanoparticle tracers, an understanding of the interaction processes between the particles and the reservoir is needed. In this study, we use DLVO, XDLVO and filtration theory to predict their behavior and identify parameters that can be adapted for design of enhanced nanoparticle-based tracers. First, we investigate the interaction between different tracer particle candidates based on DLVO theory to determine the governing factors required for dispersion stability. Once identified, the interactions of these tracer particles with typical reservoir minerals are further studied. In the next step, the filtration theory is applied to analyze the governing factors increasing the collision probability (i.e., the single grain collector contact efficiency) and to determine crucial points to consider in designing suitable tracers. The theory is examined with experimental results from flow-through tests and the advantage of surface modifiability is demonstrated. The positive effect of surface modifications is predicted by the extended DLVO (XDLVO) theory and is confirmed by flow-through experiments analyzed with filtration theory. Finally, the impact of temperature is assessed and discussed and recommendations on designing suitable nanoparticle-based tracers for geo-reservoir applications are given based on findings from DLVO, XDLVO and filtration theory.

2. Methods

2.1. DLVO theory

Dispersion stability of colloids in an aqueous media can be predicted based on DLVO theory (Agmo Hernández, 2023). The DLVO theory (named after the investigators Derjaguin, Landau, Verwey and Overbeek) adds the attractive and repulsive forces acting on the nanometer scale mutually between particles. Attractive force is the London-van der Waals force (LvdW), while repulsive force is comprised of electric double layer force (EDL) and occasionally Born repulsive force. The resulting overall force acting on spherical particles or surfaces can be attractive (negative) or repulsive (positive). When the separation distance between the objects is below approx. 0.5 nm, the repulsive Born force dominates, which originates from overlapping atomic orbitals (Christenson, 1988). Above that distance, whether the EDL or the LvdW force dominates depends on the magnitude of the EDL force. The DLVO is displayed as the resulting energy over the inter-particle distance. Its possible results are:

- A primary energy minimum
- A primary minimum and an energy barrier
- A primary minimum, an energy barrier and a secondary minimum

The depth of the primary minimum is an indication of the stability of aggregation. The deeper the primary minimum, the less likely is reversibility of aggregation. The height of the energy barrier, on the other hand, indicates the stability of the dispersion. This means, the higher the energy barrier is, the less likely is formation of aggregates and the more probable is a stable dispersion. The importance of the secondary minimum is related to its depth. The relationship is as follows: the deeper the minimum in the attractive region (i.e., values below 0), the more likely is (reversible) aggregation of particles in the secondary minimum (Elimelech et al., 1995).

DLVO forces are calculated according to Elimelech et al. (1995), Gregory (1981), Hogg et al. (1966), Muneer et al. (2020) and Ruckenstein and Prieve (1976):

$$V_{DLVO} = V_{LvdW} + V_{EDL} + V_B \quad (1)$$

$$V_{LvdW} = -\frac{A_H r}{12h} \quad (2)$$

$$V_{LvdW} = -\frac{A_H r}{6h} \quad (3)$$

$$V_{EDL} = \pi \epsilon_0 \epsilon_r \frac{r_1 r_2}{r_1 + r_2} \left[2\zeta_1 \zeta_2 \ln \left(\frac{1 + e^{-\kappa h}}{1 - e^{-\kappa h}} \right) + (\zeta_1^2 + \zeta_2^2) \ln(1 - e^{-2\kappa h}) \right] \quad (4)$$

$$V_B = \frac{A_H r \sigma^6}{1260h} \quad (5)$$

Eq. (2) describes the LvdW force between two particles and Eq. (3) between a particle and a surface. The Debye length can be calculated as:

$$\kappa^{-1} = \frac{1}{\sqrt{8\pi\lambda_B N_A 10^{-24} I}}} \quad (6)$$

With A_H being the material-dependent Hamaker constant, r particle radius, h separation distance, ϵ_r and ϵ_0 relative permittivity of medium and absolute permittivity of vacuum, respectively, $\zeta_{1,2}$ ζ -potential of interacting particles/surfaces, σ Born collision diameter, N_A Avogadro constant, λ_B Bjerrum length of fluid and I molarity of the solvent (Supplementary Table S1). ζ -potentials of silica and titania nanoparticles are taken from Spitzmüller et al. (2024b). Hamaker constants were used from literature data for the interaction of particle-particle and particle-surface in water. The constants used for the following calculations are displayed in Table 1.

2.2. Filtration theory

The single grain collector contact efficiency is calculated based on an approach by Tufenkji and Elimelech (2004) to assess the deposition of particles in porous media. Here, the porous media is assumed to consist of multiple so-called single grain collectors, which are defined as being spherical. Three different factors can be calculated: the single grain collector contact efficiency, the attachment efficiency and the single grain collector removal efficiency. They describe the probability of collision of particles with the single grain collector, the efficiency of (irreversible) attachment upon collision and the actual removal efficiency of the single grain collectors, respectively (Elimelech et al., 1995). The single grain collector contact efficiency (η_0) of particles in porous media can be described theoretically as the sum of three different mechanisms: diffusion (η_D), interception (η_I) and gravity (η_G). Single grain collector contact (η_0), removal (η) and attachment (α) efficiencies

can be calculated following the numerical solutions of the convective-diffusion equation by Tufenkji and Elimelech (2004) that also includes the contribution of hydrodynamic interactions and van der Waals attraction:

$$\eta_0 = \eta_D + \eta_I + \eta_G \quad (7)$$

$$\eta_0 = 2.4A_S^{\frac{1}{3}}N_R^{-0.081}N_{Pe}^{-0.715} + 0.55A_SN_R^{1.675}N_{Att}^{-0.125} + 0.22N_R^{-0.24}N_G^{1.11}N_{vdW}^{-0.053} \quad (8)$$

$$\eta = \alpha\eta_0 \quad (9)$$

$$\alpha = \frac{2}{3} \frac{d_c}{(1-f)L\eta_0} \ln \left(\frac{C}{C_0} \right) \quad (10)$$

with d_c collector grain size, f porosity, C/C_0 ratio of recovered particle concentration to initial concentration derived from flow-through experiments. Other parameters are:

$$N_R = \frac{d_p}{d_c} \quad \text{Aspect ratio} \quad (11)$$

$$N_{Pe} = \frac{Ud_c}{D} \quad \text{Péclet number} \quad (12)$$

$$D = \frac{k_B T}{6\pi\mu r} \quad \text{Diffusion coefficient} \quad (13)$$

$$N_{vdW} = \frac{A_H}{k_B T} \quad \text{Van der Waals number} \quad (14)$$

$$N_{Att} = \frac{A_H}{12\pi\mu r_p^2 U} \quad \text{Attraction number} \quad (15)$$

$$N_G = \frac{r_p^2 (\rho_p - \rho_f) g}{\mu U} \quad \text{Gravity number} \quad (16)$$

$$A_S = \frac{2 \left(1 - ((1-f)^{\frac{1}{3}})^5 \right)}{2 - 3(1-f)^{\frac{1}{3}} + 3((1-f)^{\frac{1}{3}})^5 - 2((1-f)^{\frac{1}{3}})^6} \quad \text{Porosity dependent number} \quad (17)$$

with d_c and d_p collector and particle size, respectively. U fluid velocity, k_B Boltzmann constant, T absolute temperature, r_p particle radius, μ viscosity, A_H Hamaker constant, ρ_p and ρ_f density of particle and fluid, respectively, g gravitational constant and f porosity. The porosity-dependent number is based on Happel's sphere-in-cell model (Elimelech et al., 1995). It should be noted that the calculations of the filtration theory do not consider the effect of a repulsive energy barrier between the single grain collector and the particle.

2.3. XDLVO theory

Nanoparticles offer the possibility of surface modifications, for example, by physi- or chemisorption of surfactants/ligands. Their presence impacts the interaction between particles and surfaces and particles with other particles. The stabilization effect of such surface modifications is usually described as steric stabilization and can be calculated by the addition of steric force to the DLVO forces:

$$V_t = V_{DLVO} + V_o + V_e \quad (18)$$

with osmotic and elastic forces calculated by piece-wise functions according to Tran and Richmond (2021), Vincent et al. (1986) and Worthen et al. (2016):

$$V_o = 0 \quad \text{If } 2L \leq h \quad (19)$$

Table 1

Hamaker constants used for calculations.

Particle-particle (in water)	Hamaker constant A_H in 10^{-20} J	Reference
Silica-Silica	0.63	Bergström (1997)
Titania-Titania	5.65	Bergström (1997)
Polystyrene-Polystyrene	0.77	French et al. (2007)
Gold-Gold	12.6	Pinchuk and Jiang (2015)
Particle-surface (in water)	Hamaker constant A_H in 10^{-20} J	Reference
Silica-Silica	0.63	Bergström (1997)
Silica-Mica	1.16	Bergström (1997)
Silica-Calcite	0.69	Bergström (1997)
Silica-Alumina	1.83	Bergström (1997)
Titania-Silica	0.69	Bergström (1997)
Titania-Mica	1.83	Bergström (1997)
Titania-Alumina	3.11	Bergström (1997)

$$V_o = \frac{4\pi r}{\nu_1} \Phi_p^2 \left(\frac{1}{2} - \chi \right) \left(L - \frac{h}{2} \right)^2 \quad \text{If } L \leq h < 2L \quad (20)$$

$$V_o = \frac{4\pi r}{\nu_1} \Phi_p^2 \left(\frac{1}{2} - \chi \right) L^2 \left(\frac{h}{2L} - \frac{1}{4} - \ln \left(\frac{h}{L} \right) \right) \quad \text{If } h < L \quad (21)$$

$$V_e = 0 \quad \text{If } L \leq h \quad (22)$$

$$V_e = \frac{2\pi r}{M_w} \Phi_p L^2 \rho_p \left[\frac{h}{L} \ln \left(\frac{h}{L} \left(\frac{3 - \frac{h}{L}}{2} \right)^2 \right) - 6 \ln \left(\frac{3 - \frac{h}{L}}{2} \right) + 3 \left(1 + \frac{h}{L} \right) \right] \quad \text{If } L > h \quad (23)$$

with r particle radius, ν_1 volume of one solvent molecule, h separation distance, Φ_p volume fraction of surfactant/ligand/polymer, L length of surfactant/ligand/polymer, M_w molecular weight of surfactant/ligand/polymer, ρ_p density of ligand and χ Flory-Huggins parameter. χ describes the compatibility of the surfactant and the solvent, with $\chi < 0.5$ being compatible and $\chi > 0.5$ incompatible.

3. Results and discussion

In the following section, the crucial factors for the design of nanoparticle tracers are indicated and discussed. First, the focus is on maintaining a stable dispersion that prevents aggregation of particles and pore-clogging by aggregates in reservoirs. Then, the interaction of selected nanoparticle tracer candidates is assessed regarding their sorption tendency toward selected reservoir minerals. In the next step,

the filtration theory is applied to analyze the governing factors that increase the collision probability and thus the nanoparticle tracer retention rate in porous media. The theory is compared with experimental results from flow-through tests and the advantage of surface modifiability of nanoparticles is demonstrated. The effect of surface modifications is predicted by the extended DLVO (XDLVO) theory and is confirmed by experimental flow-through tests analyzed with filtration theory. Finally, the impact of temperature is assessed and discussed in the framework of possible intended applications within geothermal reservoirs.

3.1. Dispersion stability – DLVO particle-particle interaction

Stable dispersions are pivotal for multiple applications, such as stable nanofluids for enhanced oil recovery (Muneer et al., 2022) or dispersed colloids for tracer tests (Berson et al., 2024) to prevent particle aggregations that could lead to pore-clogging. The dispersion stability can be assessed through calculation and interpretation of the total interaction energy (V_t) between two (spherical) particles. As shown before, V_t (Eq. (1)) is the sum of the contributions of the LvdW force (Eq. (2)), electric double layer (EDL) force (Eq. (4)) and Born force (Eq. (5))

Fig. 1 shows various DLVO interaction profiles and elucidates the impact of the parameters used for the calculations. Factors impacting the overall DLVO interaction are pH value and salinity of the solution, ζ -potential and size of the particles and the Hamaker of the particles. Generally, a rule of thumb when interpreting DLVO interaction curves is that the shallower the primary minimum, the less stable aggregation could occur. On the other hand, the higher the energy barrier, the greater the dispersion stability is, i.e., the less likely the particles are to

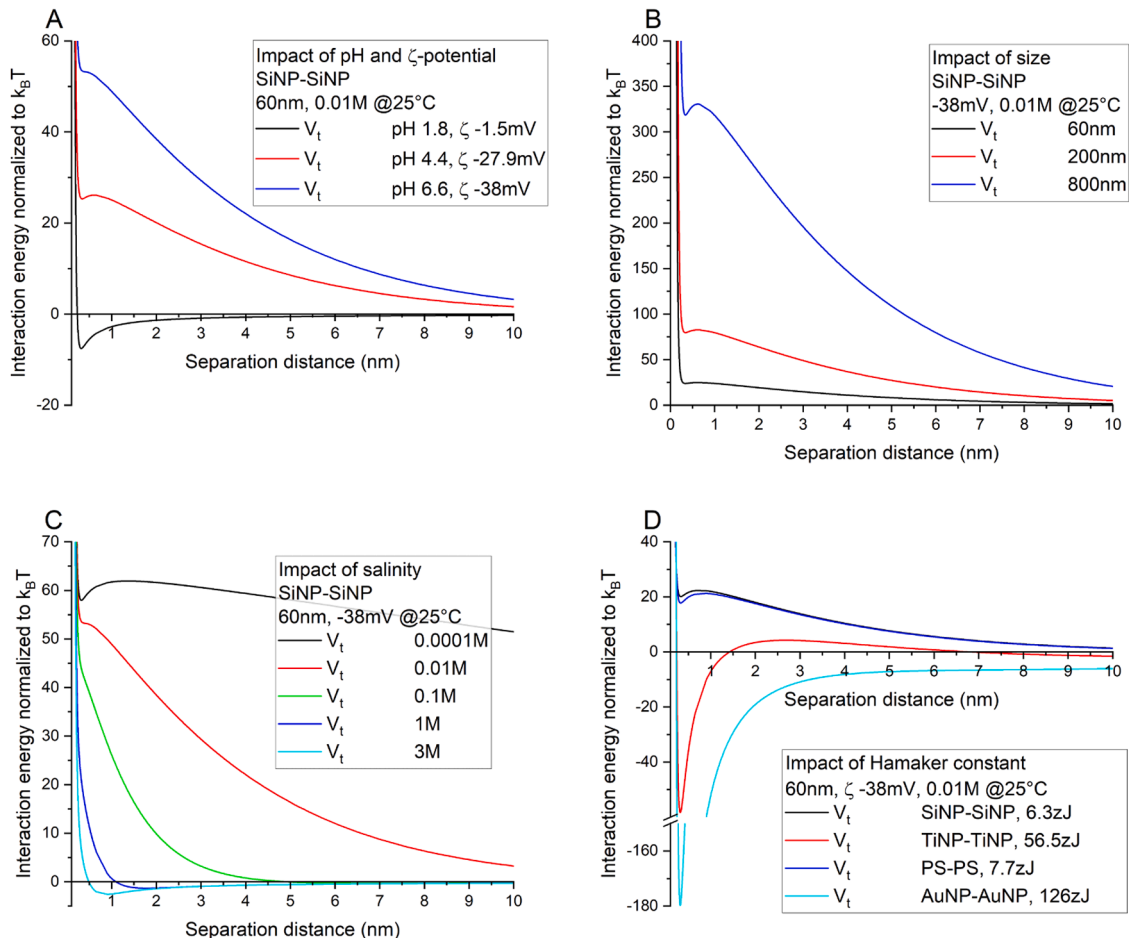


Fig. 1. DLVO interaction calculation for particle-particle. Impact of ζ -potential (A), size (B), salinity (C) and Hamaker constant (D). Note the y-axis scaling break in D.

aggregate.

Fig. 1A shows the impact of pH and the ζ -potential of the particles on 60 nm-sized silica nanoparticles in 0.01 M 1:1 electrolyte at 25 °C. It can be seen that higher ζ -potentials lead to the formation of an energy barrier and hence, dispersion stability is increased. Lower pH values that lead to near-neutral ζ -potentials are located near the so-called isoelectric point (IEP), where the resulting surface charge of particles is net-neutral. It can be seen that the further away the pH of the IEP, the more stable the dispersion as the energy barrier increases with increasing pH values and hence increasing absolute ζ -potential. The ζ -potential/pH-values impact the EDL force directly (Eq. (3)). Fig. 1B shows the impact of the size of the particle while maintaining pH/ ζ -potential, salinity, material and temperature constant. It is noticeable that increasing the size of the particles also increases the energy barrier. Further, the size of particles could also affect the ζ -potential and increase the risk of gravitational settling, which is neglected in this calculation. The size of the particles affects all three forces (LvdW force, EDL force and Born force, Eqs. (2)–(5)). The impact of salinity in a 1:1 electrolyte is shown in Fig. 1C while maintaining pH/ ζ -potential, size, material and temperature constant. Lower salinity leads to a higher energy barrier. This behavior is attributed to increased EDL force caused by the increase of the Debye length, which inversely depends on salinity. Contrarily, when salinity increases, the Debye length decreases. Hence, the EDL force range is short, which, in turn, results in attractive force overpowering repulsive force. Thus, the energy barrier is lowered or even an attractive primary minimum appears (as in Fig. 1C 3M case) that lowers the dispersion stability drastically. Fig. 1D points out the impact of nanoparticle material represented as a change in the Hamaker constant (individual interaction constant for materials within a medium, i.e., water, values see Table 1). All other factors are kept constant to elucidate the impact of the nanoparticle material: 60 nm-sized particles, pH/ ζ -potential constant, 0.01 M 1:1 electrolyte and 25 °C. Tested cases are silica, titania, polystyrene/latex and gold nanoparticles with A_H $6.3 \cdot 10^{-21}$ J, $5.65 \cdot 10^{-20}$ J, $7.7 \cdot 10^{-21}$ J and $1.26 \cdot 10^{-19}$ J, respectively. The Hamaker constant contributes to the Born repulsive force (Eq. (5)) and the London-van der Waals attractive force (Eq. (2)). It can be seen that increasing values lead to the formation of a deep primary minimum, i.e., the London-van der Waals force outweighs the repulsive EDL force. However, it should be remarked that nanoscale roughness can affect the Hamaker constant, leading to reduced attractive force and, hence, additionally stabilizing the particle dispersion (Valmacco et al., 2016).

In general, colloidal dispersions are stable when the resulting interaction energy based on DLVO theory is positive, i.e., repulsive. This is primarily the case when the particles have ζ -potentials of the same sign, when the fluid's salinity is low and when the material-dependent Hamaker constant is small. The resulting overall interaction energy is an interplay of many factors. Silica nanoparticles have sufficiently low Hamaker constants and form stable dispersions below 0.1 M salinity. The ζ -potential should be far from the IEP, i.e., pH values should be significantly higher or lower. As a general recommendation, nanotracers should preferably be made out of silica or polystyrene but not (entirely) metallic. However, it should be noted that these calculations represent isolated calculations with only one variable. In reality, sizes, temperatures, pressure, material and salinity also impact ζ -potential and Hamaker constant values (e.g., Pinchuk and Jiang (2015)). Therefore, the calculations presented here are simplified but serve to obtain a first-order impression on dispersion stability.

3.2. Sorption tendency – DLVO particle-surface interaction

When nanoparticles are used as tracers in natural environments, their interaction with reservoir mineral surfaces is crucial in determining their overall performance, particularly their tendency for sorption and retention. The DLVO theory is applied to assess these interactions between silica and titania nanoparticles and four different rock surfaces — silica, mica, calcite, and alumina — chosen for their

significantly varying ζ -potentials. Mica has the most negative ζ -potential at -70 mV (Zaucha et al., 2011), followed by silica with a ζ -potential of -30 mV (Hartmann et al., 2018) and the most positive is alumina with +40 mV (Izrael-Zivković et al., 2015). For calcite, the span of ζ -potential found in literature is vast. However, to represent an intermediate value, a ζ -potential of -5 mV is chosen from data by Al Mahrouqi et al. (2017). The ζ -potentials of silica and titania nanoparticles were measured with a ζ -sizer and are valid for 0.01 M 1:1 salt solutions at ambient temperatures (Spitzmüller et al., 2024b). To calculate the attractive London-van der Waals force, Hamaker constants are employed. The specific values used in calculations and their references are listed in Table 1. For the titania-water calcite system, the Hamaker constant is assumed to be similar to that of the titania-water-mica system.

Fig. 2 illustrates the DLVO interactions between the silica and titania nanoparticles and the surfaces. For silica nanoparticles, an energy barrier is observed in interactions with mica (A) and silica (B). The height of the energy barrier depends on the value of the ζ -potential with SiNP-mica owing the highest energy barrier. Interestingly, the interaction of silica nanoparticles with calcite (C) leads to the formation of a small and negative “energy barrier” at larger separation distances of about 5 nm. As expected, when interacting with alumina (D) no energy barrier forms due to the opposite charges between the negatively charged SiNPs and positively charged alumina surface, resulting in a deep primary minimum that indicates strong adsorption.

For positively charged titania nanoparticles, the behavior contrasts with silica nanoparticles. Deep primary minima and no energy barriers are observed in interactions with mica, silica, and calcite (A, B, C). However, in the interaction with the positively charged alumina surface (D), an energy barrier appears. Compared to the interaction of SiNPs with mica and silica, the energy barrier is relatively small and the primary minimum is deeper. This behavior is attributed to the near-neutral ζ -potential of the TiNPs, which are below the threshold of ± 30 mV for stable dispersion and to the Hamaker constant of $3.11 \cdot 10^{-20}$ J, which is higher than for the other interactions. As shown before, higher Hamaker constants increase the London-van der Waals force to exceed possibly the repulsive EDL force. Although having the same sign, attraction dominates between titania and the alumina surface at short separation distances.

In most cases, the silica nanoparticles are superior to the positively charged titania nanoparticles due to the predominantly negative charges of most natural minerals and reservoir rocks (Walker and Glover, 2018). Therefore, having a nanoparticle tracer with negative charges is more likely to have less sorption tendency than a positively charged tracer. It should be noted, however, that the salinity of the fluids is of great importance for the dispersion stability and sorption tendency. Especially for geothermal environments where salinity can reach up to several hundred grams per liter (Sanjuan et al., 2016), maintaining a high surface potential is crucial. As the Debye length is affected by the salinity, the effect of the repulsive EDL force is rather low and might not suffice to overcome the London-van der Waals force. However, it is shown that especially polyvalent ions might have a greater impact on dispersion stability than the level of salinity (Xie et al., 2016). For example, divalent ions, in general, increase the ionic strength, thus reducing the Debye length and, therefore, lowering the EDL forces (Muneer et al., 2020). Furthermore, divalent ions greatly influence the ζ -potential, as this value also depends on the ionic strength. Additionally, it should be noted here that the classical DLVO does not account for the impact of hydration of the ions (Ninham, 1999). For example, cesium is experimentally proven to affect the interaction to a greater extent than sodium at the same concentration, although both are monovalent ions (Wang et al., 2013). Their effect on dispersion stability can be best described by reversed or direct Hofmeister series (Ninham, 1999).

In conclusion, negatively charged silica nanoparticles typically form energy barriers when interacting with the selected surfaces, reducing their sorption tendency. Positively charged titania nanoparticles generally do not form energy barriers, leading to a higher sorption

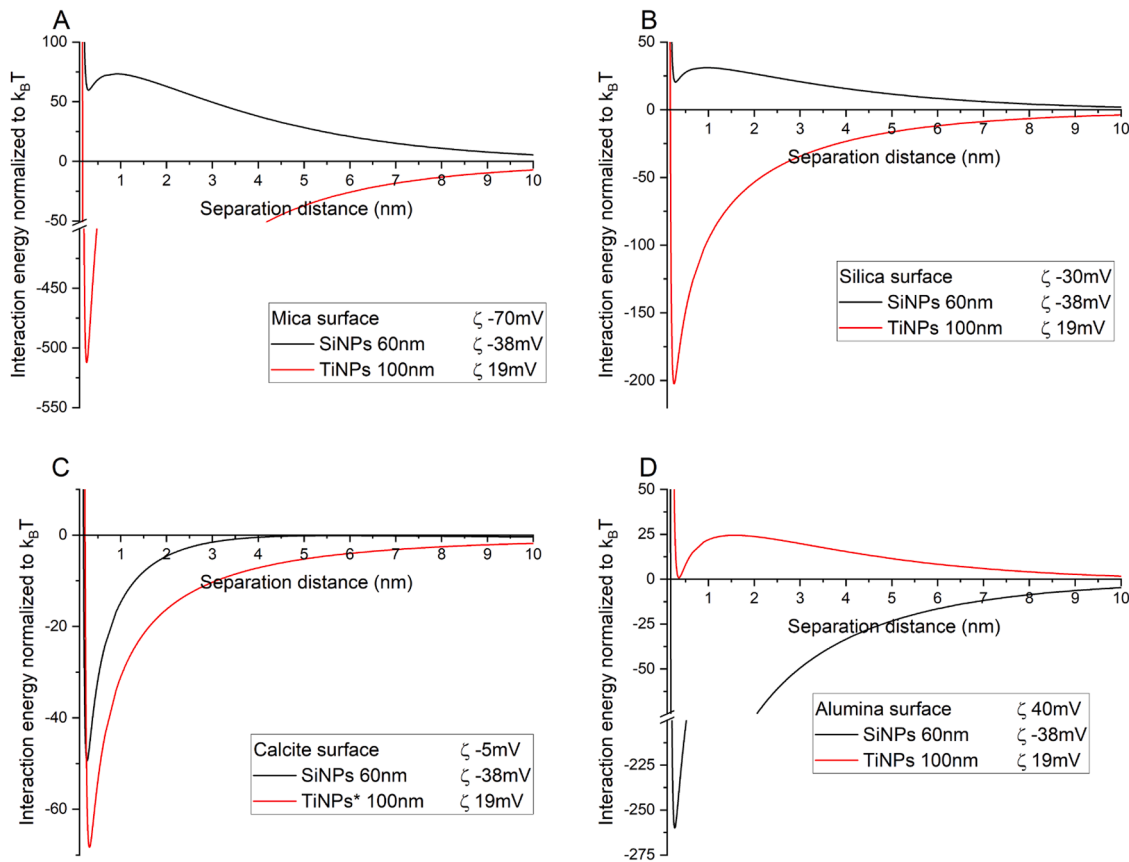


Fig. 2. DLVO interaction calculations for particles-surfaces. * Hamaker constant for titania-water-mica used. Note the y-axis scaling break in A and D.

tendency in most cases, unless the mineral surfaces are also positively charged.

3.3. Predictions of particle deposition based on filtration theory

Filtration theory can be used to assess the probability of particle deposition within a porous medium. The correlation-equation derived by Tufenkji and Elimelech (2004) accounts for the contribution of three different processes on the overall single grain collector contact efficiency (see Eq. (8)): Diffusion, interception and gravity (gravitational settlement). For calculation, the single grain collector size is kept constant at 1 mm and the density of the particles is assumed to be 1.6 g/cm³ (a typical value for SiNPs (Qiao et al., 2009; Silencieux et al., 2015)). The Hamaker constant is 6.9·10⁻²¹J (titania-water-silica interaction, considered as representative for dye-MSN@TiO₂ tracer particles). Porosity of the flow system is set to 35 % (Berson et al., 2024).

Fig. 3A shows the contribution of each of the physical fluid dynamic parameters in dependence of flow velocity and particle size. To facilitate better categorization of the flow velocities: the mean flow velocities determined by tracer tests in the geothermal system Soultz-sous-Forêts (France) range between 3.7·10⁻⁵ m/s (3.2 m/d) and 2.25·10⁻³ m/s (194.4 m/d) (Radilla et al., 2012; Sanjuan et al., 2006). In Fig. 3, η_0 , as well as individual contributions of diffusion, interception and gravity, are shown in dependence of particle size. Reaching a probability of collision of unity means 100 % of particles will collide with the single grain collector. In Fig. 3A-D, the impact of variation in fluid velocity is shown as well. Two main trends can be identified: Diffusion is the governing mechanism at decreasing particle size and a lower flow rate increases the probability of collision independent of particle size. The impact of gravity diminishes drastically with increasing fluid velocity and is more dependent on velocity than particle size, although increasing particle size increases gravitational settling. Interception

depends rather on particle size than on fluid velocity. The lowest probability of collision is in all cases shown in Fig. 3 in the lower range of μ -sized particles. The probability of collision increases drastically with decreasing particle size due to the contribution of diffusion-dominated collisions and increases with increasing particle size due to the contribution of interception and gravity.

Fig. 4 demonstrates the impact of particle size and fluid velocity on the probability of collisions. The parameters are equal to those used for calculations displayed in Fig. 3, but here, they are shown in dependence on fluid velocity. It can be seen that for particle sizes 50 nm and 500 nm, the single grain collector contact efficiency (η_0) is governed solely by diffusion, whereas for the 5000 nm (5 μ m) particles, interception dominates at higher flow rates. In the case of 50,000 nm (500 μ m)-sized particles, the dominant mechanism at low flow rate is gravity and at flow rates above 10⁻⁵ m/s interception.

For calculations shown in Figs. 3 and 4, the size of the particle collector was kept constant at 1 mm, which is in the range of coarse sand. Fig. 5 shows the impact of the collector grain size on the collision probability. Fig. 5 shows the impact of varying collector size from 1 μ m to 1000 μ m (1mm) for particle sizes of 150 nm (Fig. 5A) and 1000 nm (Fig. 5B) with a density of 1.6 g/cm³, A_H 6.9·10⁻²¹J at constant fluid velocity of 3.8·10⁻³ m/s. For 150 nm particles and collector sizes below 10 μ m, the dominant mechanism for collision is interception.

Above 10 μ m, the dominant mechanism is diffusion, as was anticipated by calculations presented in Figs. 3 and 4. The unexpected dominance of interception at collector grain sizes below 10 μ m can be explained by straining, i.e., size exclusion. According to Xu et al. (2006), the limit for straining to occur is at a particle-to-collector size ratio of above 0.008. In the case of 150 nm particles and 1 μ m collector grain, this ratio is 0.15, which means that straining is likely to contribute to particle deposition/retention. It should be noted that Eq. (8) does not accomplish the impact of straining and η_0 values are inaccurate at these

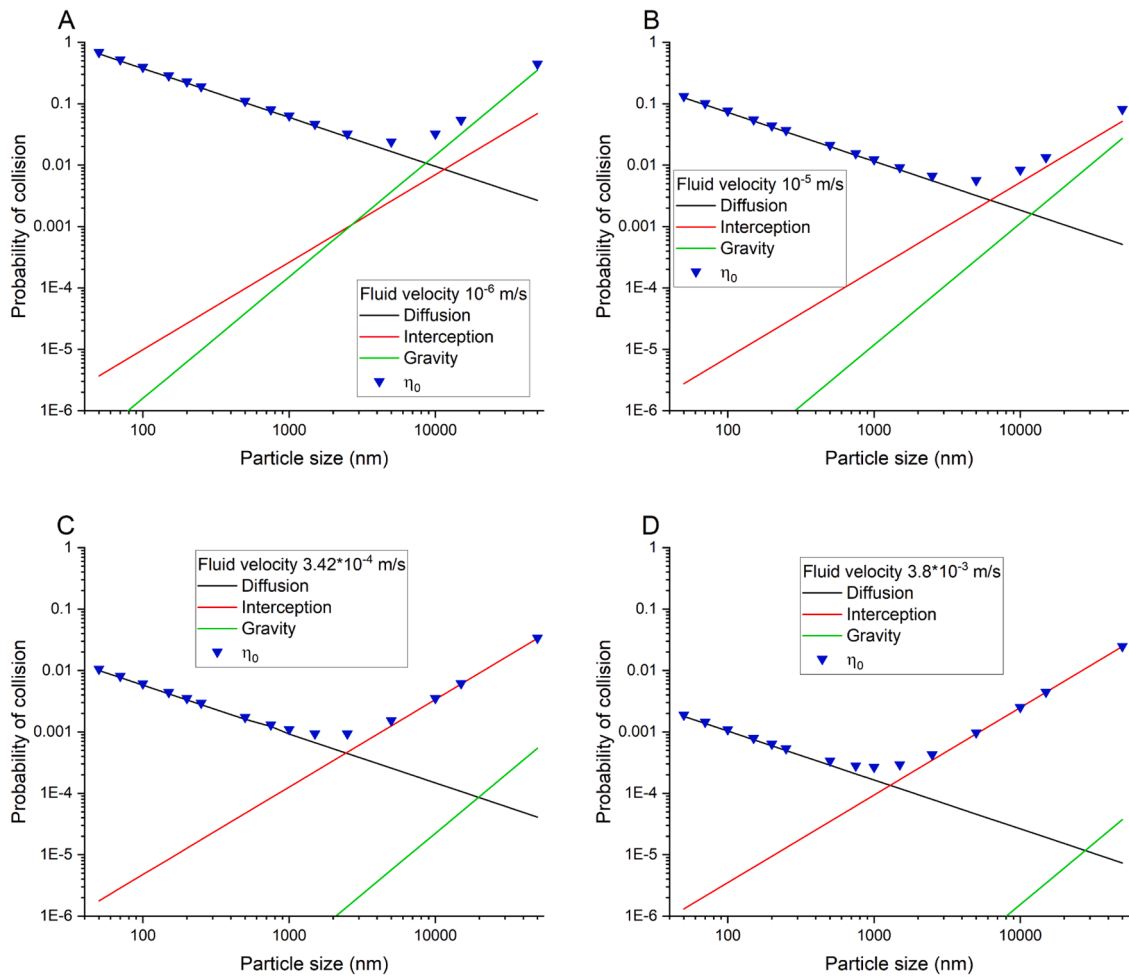


Fig. 3. Factors contribution to the single grain collector contact efficiency η_0 in dependence of particle size. Collector size 1 mm, density 1.6 g/cm³, A_H 6.9•10⁻²¹ J, porosity 35 %.

conditions (Bradford et al., 2002).

For 1000 nm (1 μ m) particles, the behavior is principally similar to the 150 nm particles: at low particle-to-collector ratios, the dominant mechanism seems to be interception. Up to a collector size of approx. 500 μ m (collector/particle 0.002) interception is the dominant mechanism above that diffusion dominates. Although the impact of gravity is increased, it is still orders of magnitudes lower than the impact of interception and diffusion. η_0 is mostly overestimated. Consequently, for calculations of the actual single grain removal efficiency (η), η_0 is adapted by multiplication with a factor called the attachment efficiency α that is derived from experimental data. In calculated η values have been calculated by multiplication of η_0 with attachment efficiencies (α) determined by flow-through experiments (Berson et al., 2024; Rudolph, 2021; Spitzmüller et al., 2023a). The particle size is 60 nm, collector size 1 mm, porosity 35 %, the density of the particles is approx. 2 g/cm³ and the Hamaker constant is 6.3•10⁻²¹ J (Table 1).

In Fig. 6A, the single grain collector contact efficiency (η) is shown as a function of salinity with increasing salinity resulting in increased collision probability. By adding the anionic surfactant SDS or the zwitterionic surfactant SB3-14, the attachment efficiency is lowered and hence η is lowered. In Fig. 6B, these data points (at a salinity of 0.17 M) are plotted in a collision probability diagram and compared to η_0 values and the three main removal mechanisms. It can be seen that the governing mechanism for particle deposition at the used particle size (60 nm) is diffusion. However, the η -values for the experiments are lower than the expected η_0 values (Fig. 6B). That means the attachment efficiency (α) must therefore be lower than unity (<100 %), which implies

that not all collisions lead to attachment. Similar to these results, lower than predicted attachments were also lower than seen in several other studies (Elimelech et al., 1995; Elimelech and O'Melia, 1990; Hull and Kitchener, 1969; Marshall and Kitchener, 1966). This discrepancy was attributed either to surface charge heterogeneity or to a repulsive double layer (and hence an energy barrier). In this experimental setup with SiNPs and quartz sand, DLVO theory predicts the formation of a repulsive barrier between silica and quartz sand. It should be noted that if the attractive forces described in the DLVO theory govern colloidal retention/filtration, the salinity of the fluids could play an important role. On the other hand, if filtration/retention of particles is rather caused by hydraulics, it is mostly independent of ionic strength (Carstens et al., 2019).

For the experiments with additives, the η is even lower, which indicates that the attachment efficiency is further decreased due to the presence of the additives (Tian et al., 2010). The anionic surfactant shows the highest impact on lowering the attachment efficiency and, hence, the probability of collision. An explanation for the behavior cannot be found in the traditional DLVO theory as it does not account for steric factors. This requirement elaboration is augmented in the XDLVO theory.

3.4. The importance of XDLVO theory: adding a steric barrier

As shown in Fig. 6, adding surfactants that physisorb on the surface of the nanoparticles changes the attachment efficiency (and single grain collector removal efficiency). An explanation is given by the XDLVO

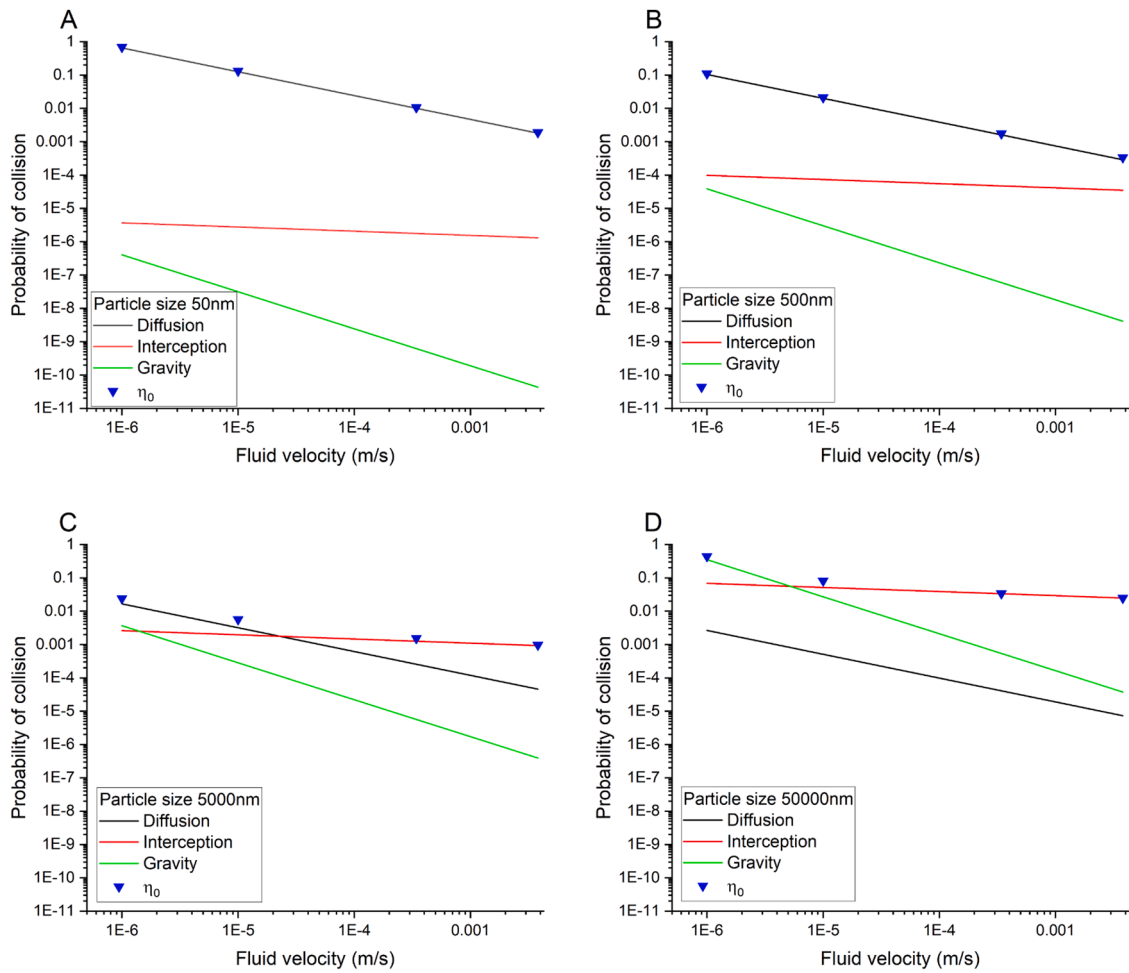


Fig. 4. Factors contribution to single grain collector contact efficiency η_0 and overall probability of collision in dependence particle size and flow velocity. Collector size 1 mm, density particles 1.6g/cm³, A_H 6.9•10⁻²¹J, porosity 35 %.

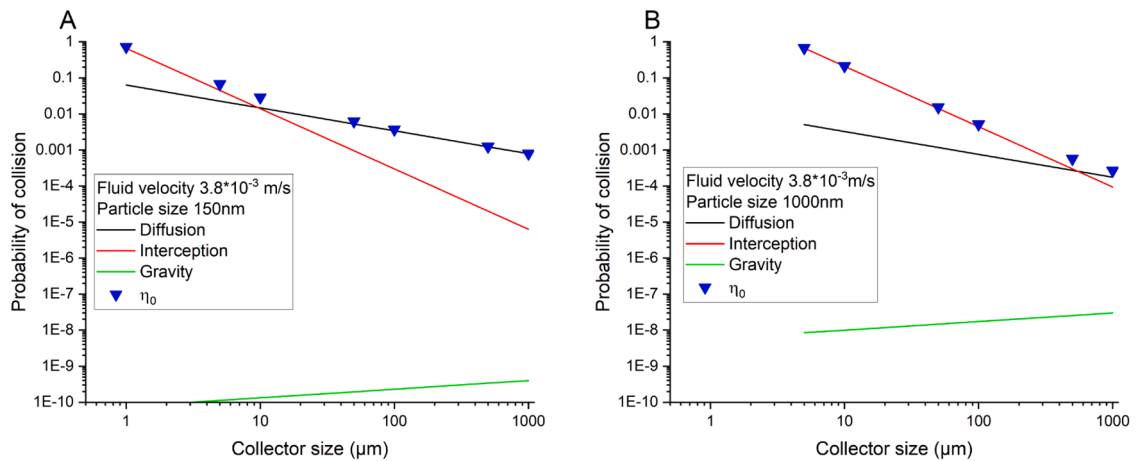


Fig. 5. Impact of collector size on probability of collision. A) particle size 150 nm, B) particle size 1 μm. As size exclusion effects are not considered in Eq. (8), estimation of η_0 for particle/collector ratio above 0.008 is not sufficiently accurate (Auset and Keller, 2006; Xu et al., 2006).

theory: the surfactants form a steric barrier and increase the repulsive force, thus creating an energy barrier (Napper and Netschey, 1971; Zhulina et al., 1990).

Here, calculations on the impact of such a steric barrier are made according to XDLVO theory for the zwitterionic SB3-14 surfactant on dye-MSN@TiO₂ nanotracers developed by Spitzmüller et al. (2024a).

Four different cases are chosen to determine the effect of the steric barrier: Particle-particle and particle-surface interactions with three different surfaces - silica, alumina and mica. For the calculations, RhB-MSN@TiO₂ nanoparticles are used with a size of 150 nm with added 0.1 mg/mL of zwitterionic surfactant SB3-14 and a ζ -potential of +19 mV at pH 6.6 in 10 mM KCl at 25 °C. ζ -potentials for the surfaces are

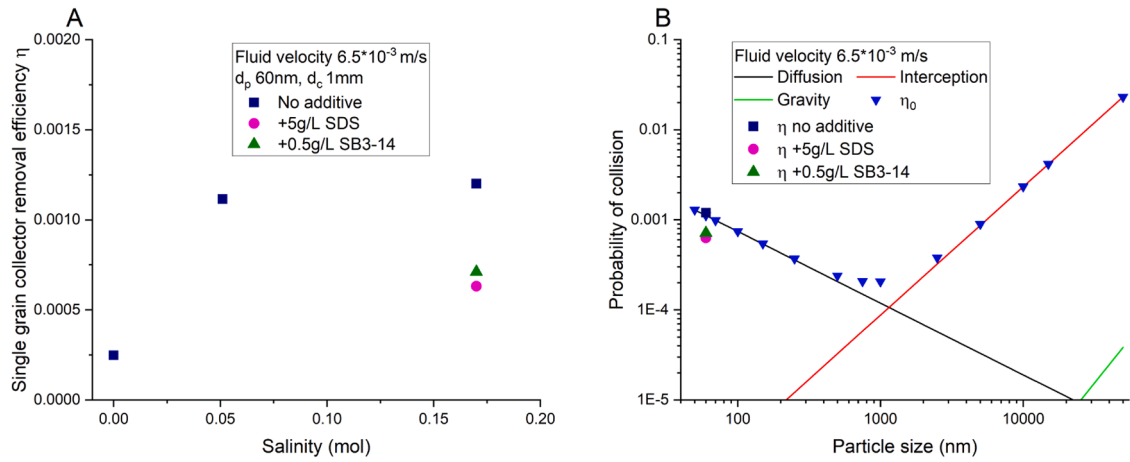


Fig. 6. A) Single grain collector removal efficiency η in dependence of salinity. α calculated using data from flow-through experiments by Berson et al. (2024), Rudolph (2021) and Spitzmüller et al. (2023a). Impact of additives is shown by effectively lowering the removal efficiency. B) Probability of collision and impact of diffusion, interception and gravity. η calculated according Eq. (8).

-70 mV, -30 mV and +40 mV for mica, silica and alumina, respectively (Hartmann et al., 2018; Izrael-Živković et al., 2015; Zaucha et al., 2011). Hamaker constants for the interactions are chosen according to Table 1 for titania interactions.

Fig. 7 shows the DLVO forces in black and the XDLVO forces in red, green and blue for varying Flory-Huggins χ -parameter. The χ -parameter indicates the compatibility of the surfactant with the surrounding media (water). Values below 0.5 indicate compatibility, with smaller values showing increasing compatibility and values above 0.5 indicate incompatibility (e.g., hydrophobic particles in water). In Fig. 7

χ -parameters are therefore chosen to be highly compatible ($\chi=0.30$), slightly compatible ($\chi=0.49$) and slightly incompatible ($\chi=0.51$). The effect of incompatible surfactants/surface coating ($\chi=0.51$) is drastic: instead of forming an additional energy barrier, the depth of the primary minimum increases. As shown in Fig. 7 for $\chi=0.51$, the attraction between the particles and particles-surface is enhanced and no steric barrier is formed due to the incompatibility of the surface coating and the medium. On the other hand, with slightly compatible surfactants ($\chi=0.49$), a steric barrier is formed and its effect is further increased at $\chi=0.30$. Two significant conclusions can be drawn: The steric barrier

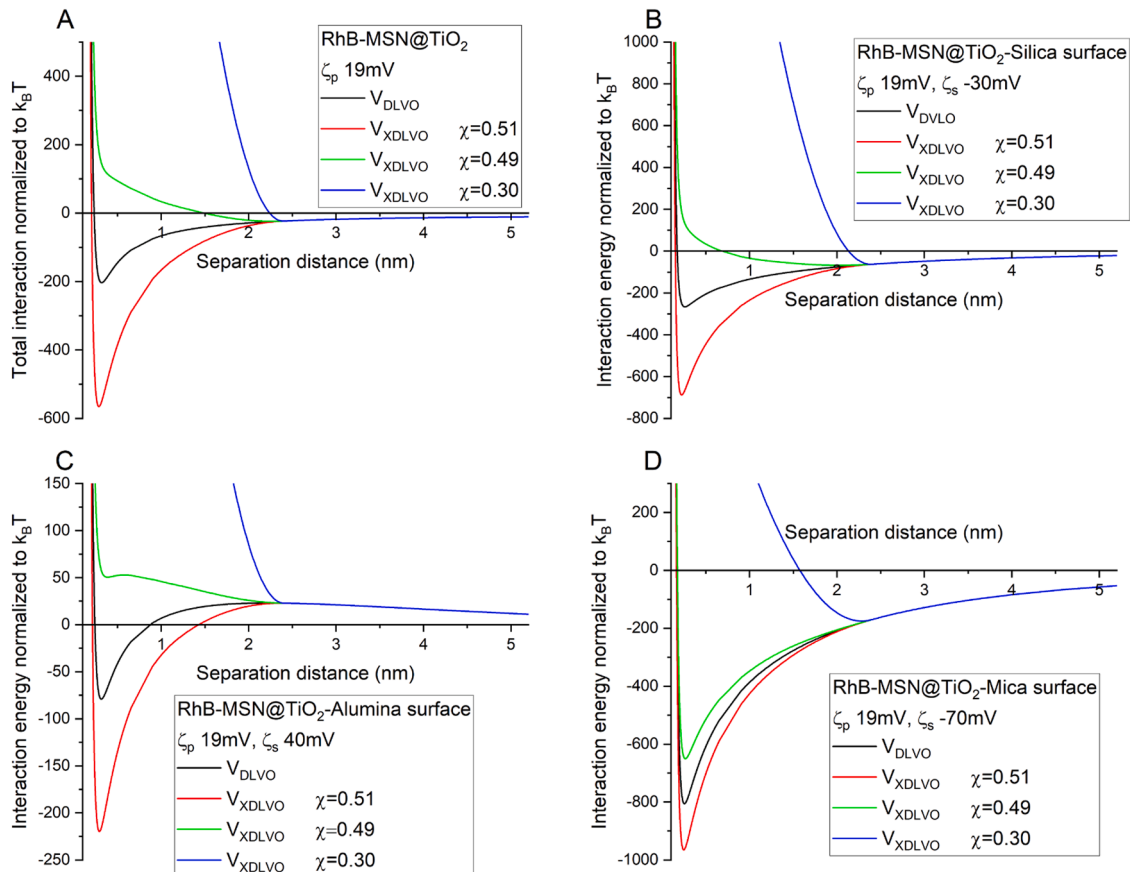


Fig. 7. XDLVO forces calculations with varying Flory-Huggins χ parameter for particle-particle interaction (A) and particle-surface interaction (B).

function only acts up to twice the length of the polymer and increases with polymer-fluid compatibility. For example, in Fig. 7D, the secondary minimum at approx. 2.5 nm is still existent and remains unaffected by the surface coating.

In this example, the surface coverage was set to be 10^{-6} mol/m² whereas in Fig. 8, this value is varied up to $5 \cdot 10^{-6}$. An energy barrier starts forming in this set-up at a surface coverage of $1.25 \cdot 10^{-6}$ mol/m², even for a Flory-Huggins value of $\chi=0.49$. Therefore, having adequate surface coverage further increases the stabilizing measure of the steric barrier. From literature data, it is anticipated that coverage of up to half of the available particle surface is ideal (Healy and La Mer, 1964).

Finally, it should be noted that the calculations made here are only exemplary with several assumptions (e.g., surface coverage, molecular weight of the polymer, χ -parameter, listed in Supplementary Table S1) and neither account for fluid salinities above 0.01 M nor temperatures above 25 °C. Consequently, the ζ -potentials are assumptions or measurements but must be considered to have uncertainties. However, calculations based on XDLVO theory show the importance and effect of surface modifications on reducing particle-particle aggregation and particle-surface adsorption.

3.5. Impact of temperature

Temperature affects multiple parameters used in (X)DLVO and filtration theory calculations, namely ζ -potential/pH, Debye length κ^{-1} due to temperature dependence of the Bjerrum length λ_B , Hamaker constant A_H , relative permittivity ϵ_r , diffusion coefficient D , viscosity μ and fluid density ρ_f (Supplementary Table S2). While the temperature dependence of most parameters is well determined, there is a lack of accurate datasets for the changes in the ζ -potential and the Hamaker constant values. While ζ -potential measurement at elevated temperatures is technically complicated, Tosha et al. (2003) established an empirical formula by experimental results (Ishido and Mizutani, 1981) to determine the temperature-dependent ζ -potential up to 150 °C. While this formula only applies to salinities below 0.01 M, increased salinity cancels the temperature dependence of the ζ -potential (Al Mahrouqi et al., 2017). In the following calculations, the ionic strength is therefore fixed to 0.01 M 1:1 electrolyte. The other unknown temperature-dependent parameter is the Hamaker constant, which can be determined following the Lifshitz approach using the permittivity of the particles and the medium as well as the frequency. Jiang and Pinchuk (2016) showed that the Hamaker constant of metal nanoparticles is size- and temperature-dependent. Lefèvre and Jolivet (2009) reported a Hamaker constant change by a factor of 2 up to temperatures of 350 °C. Barton (2019) approximated the Hamaker constant change of silica to be

1.6 from 25 °C to 100 °C. While Lefèvre and Jolivet (2009) and Ghosh et al. (2006) estimated an increase in the Hamaker constant with increasing temperature, Barton (2019) and Yan et al. (2014) predicted a decrease. We therefore assume in the following calculations that the Hamaker constant remains temperature-independent for the selected cases, which are below 100 °C. Fig. 9 shows the impact of temperature on DLVO forces and the single grain collector contact efficiency (η_0). Generally, increasing temperature increases the energy in the system, thus either increasing the risk of deposition due to increased probability of collisions (filtration theory) or decreasing the risk of deposition due to higher energy barriers (DLVO theory). In the case of DLVO forces, the energy barrier increases likely due to increased absolute ζ -potential (calculated according to Tosha et al. (2003)), although ϵ_r and κ^{-1} decrease. Simultaneously, the probability of collision increases with increasing temperature, mainly driven by increased diffusion due to the temperature-dependence of the Brownian motion (Supplementary Figure S1). However, calculations of η using results from flow-through experiments show an inhomogeneous pattern with lower-than-predicted single grain collector removal efficiencies for 45 nm particles and higher-than-predicted values for 650 nm particles. Explanations for $\eta < \eta_0$ could be the presence of an energy barrier or particle detachment, while for $\eta > \eta_0$, factors, such as particle aggregation, straining, sieving and bridging might play an important role. Comparable literature data on temperature dependence is scarce and often inhomogeneous. For example, Caldeas et al. (2011) found retention of 5 nm silica nanoparticles within porous media to increase by only 2 % at 80 °C, while Abdelfatah et al. (2017) calculated a reduced retention for the same setup. Therefore, to understand the impact of temperature more fully, additional tools like atomic force microscopy (AFM) should be employed (Wang et al., 2013).

4. Conclusions and guidelines on nanoparticle tracer design

Although the presented calculations are not comprehensive due to inaccuracies in unknown, vague or estimated parameters, such as ζ -potential, Hamaker constants and Flory-Huggins χ -parameter, an overall trend can be observed. Guidelines based on these trends in (X) DLVO and filtration theory for nanoparticle tracer design are:

- Nanoparticle material should exhibit low Hamaker constant, i.e., preferably not metallic
- Nanoparticles with (strong) negative ζ -potential are less likely to be retained within the porous media due to mostly negatively charged reservoir minerals
- Particle and surface ζ -potential should ideally have the same sign
- Particle sizes below 1 μm increase the probability of collision with mineral grains caused by increased diffusion
- Particle size needs to be adequate for the fluid velocity and the particle-to-grain size ratio should be below 0.008 to avoid size exclusion effects
- Impact of gravity on collision is mostly negligible for particle sizes below 1 μm . Therefore, a higher density of smaller nanoparticles is not detrimental
- Compatible surface modifications (i.e., $\chi < 0.5$) give rise to an additional repulsive force, stabilize colloidal dispersion due to steric stabilization and can lower attachment efficiencies
- The range of the steric force is limited to twice the length of the surfactant. Therefore, possibly multi-layer coatings could be more effective in reducing aggregation

Considering these recommendations, it is possible to design a tracer that exhibits high colloidal stability and a reduced sorption tendency. Additionally, by applying surface modifications, there is a high potential to enhance the performance of these nanoparticle tracers and improve their transport properties. To create a more comprehensive base of knowledge, further investigations are needed to accurately identify the

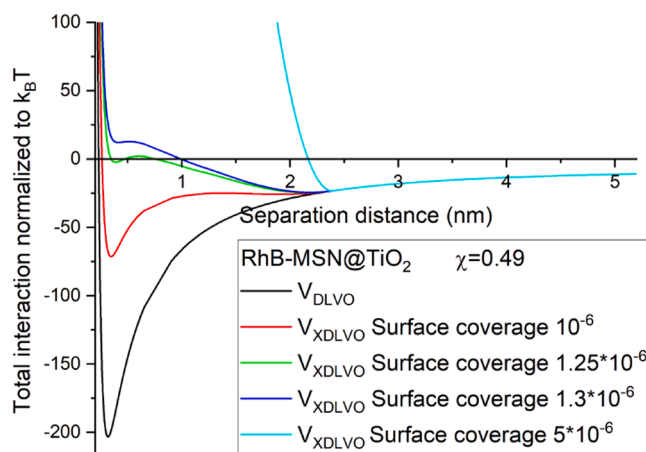


Fig. 8. Impact of surface coverage on effectiveness of steric barrier calculated using XDLVO theory.

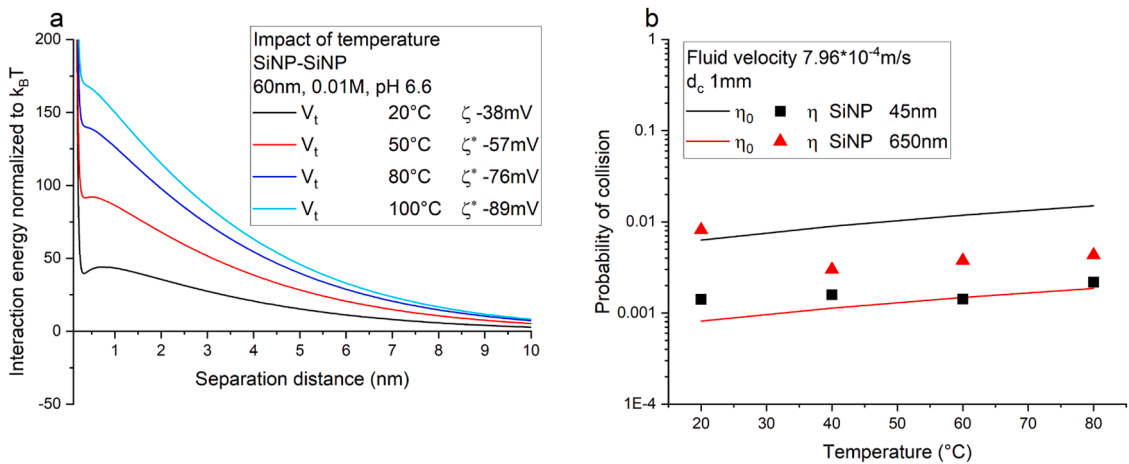


Fig. 9. Impact of temperature on DLVO theory and collision probability. η calculated using α -values from unpublished flow-through experiments at elevated temperatures * ζ -potential calculated according to the formula by Tosha et al. (2003).

impact of geothermal conditions on parameters such as ζ -potential and Hamaker constant.

Nomenclature

Abbreviation	Name
A_H	Hamaker constant
A_S	Porosity dependent number
C	Concentration
C_0	Initial concentration
D	Diffusion coefficient
d_c	Collector diameter
d_p	Particle diameter
f	Porosity
g	Gravitational constant
h	Separation distance
k_B	Boltzmann constant
L	Length of polymer/ligand/surfactant
M_W	Molecular weight
N_A	Avogadro constant
N_{Att}	Attraction number
N_G	Gravity number
N_{Pe}	Péclet number
N_R	Aspect ratio
N_{vdW}	Van der Waals number
r_p	Particle radius
T	Temperature
U	Fluid velocity
V_B	Born force
V_e	Elastic force
V_{EDL}	Electrostatic double layer force
V_{LvdW}	London-van der Waals force
V_O	Osmotic force
V_S	Steric force
V_t	Total interaction energy
α	Attachment efficiency
ϵ_0	Absolute permittivity of vacuum
ϵ_r	Relative permittivity of solvent
ζ	Zeta potential
η_0	Single grain collector contact efficiency
η	Single grain collector removal efficiency
κ^{-1}	Debye length
λ_B	Bjerrum length
μ	Viscosity
ν_1	Volume of solvent molecule
ρ	Density
σ	Born collision diameter
Φ_P	Volume fraction
χ	Flory-Huggins parameter

CRedit authorship contribution statement

Laura Spitzmüller: Writing – original draft, Visualization, Methodology, Investigation, Formal analysis, Conceptualization. **Jonathan Berson:** Writing – review & editing, Methodology, Investigation. **Thomas Kohl:** Supervision, Resources, Project administration, Funding acquisition. **Thomas Schimmel:** Supervision, Resources. **Fabian Nitschke:** Writing – review & editing, Supervision, Project administration, Conceptualization.

Declaration of competing interest

The authors declare that they have no known competing financial interests or personal relationships that could have appeared to influence the work reported in this paper.

Acknowledgements

This study is part of the subtopic “Geoenergy” in the program “MTET—Materials and Technologies for the Energy Transition” of the Helmholtz Association.

Supplementary materials

Supplementary material associated with this article can be found, in the online version, at [doi:10.1016/j.geothermics.2025.103309](https://doi.org/10.1016/j.geothermics.2025.103309).

Data availability

Data will be made available on request.

References

Abdelfatah, E.R., Kang, K., Pournik, M., Shiao, B., Harwell, J., 2017. Study of nanoparticle adsorption and release in porous media based on DLVO theory. *J. Petrol. Sci. Eng.* 157, 17. <https://doi.org/10.1016/j.petrol.2017.08.003>.
Adamczyk, Z., Weroniski, P., 1999. Application of the DLVO theory for particle deposition problems. *Adv. Colloid. Interface Sci.* 83. [https://doi.org/10.1016/S0001-8686\(99\)00009-3](https://doi.org/10.1016/S0001-8686(99)00009-3).
Agmo Hernández, V., 2023. An overview of surface forces and the DLVO theory. *ChemTexts* 9 (10). <https://doi.org/10.1007/s40828-023-00182-9>.
Al Mahrouqi, D., Vinogradov, J., Jackson, M.D., 2017. Zeta potential of artificial and natural calcite in aqueous solutions. *Adv. Colloid. Interface Sci.* 240. <https://doi.org/10.1016/j.cis.2016.12.006>.
Alaskar, M., Ames, M., Chong, L., Li, K., Horne, R., 2015. Temperature nanotracers for fractured reservoirs characterization. *J. Petrol. Sci. Eng.* 127. <https://doi.org/10.1016/j.petrol.2015.01.021>.

- Auset, M., Keller, A.A., 2006. Pore-scale visualization of colloid straining and filtration in saturated porous media using micromodels. *Water Resour. Res.* 42. <https://doi.org/10.1029/2005WR004639>.
- Barton, I., 2019. The effects of temperature and pressure on the stability of mineral colloids. *Am. J. Sci.* 319. <https://doi.org/10.2475/09.2019.01>.
- Bergström, L., 1997. Hamaker constants of inorganic materials. *Adv. Colloid. Interface Sci.* 70, 45. [https://doi.org/10.1016/S0001-8686\(97\)00003-1](https://doi.org/10.1016/S0001-8686(97)00003-1).
- Berson, J., Rudolph, B., Spitzmüller, L., Kohl, T., Schimmel, T., 2024. Reporting nanoparticle tracers: validation of performance in flow-through experiments simulating reservoir conditions. *J. Hydrol.* 637. <https://doi.org/10.1016/j.jhydrol.2024.131429>.
- Bradford, S.A., Yates, S.R., Bettahar, M., Simunek, J., 2002. Physical factors affecting the transport and fate of colloids in saturated porous media. *Water Resour. Res.* 38. <https://doi.org/10.1029/2002WR001340>.
- Caldelas, F., Murphy, M.J., Huh, C., Bryant, S.L., 2011. Factors governing distance of nanoparticle propagation in porous media. *SPE J.* <https://doi.org/10.2118/142305-MS>.
- Carstens, J.F., Bachmann, J., Neuweiler, I., 2019. A new approach to determine the relative importance of DLVO and non-DLVO colloid retention mechanisms in porous media. *Colloids Surf. A: Physicochem. Eng. Aspects* 560. <https://doi.org/10.1016/j.colsurfa.2018.10.013>.
- Chakraborty, S., Elhaj, R., Foppen, J.W., Schijven, J., 2023. Effect of injection water ionic strength on estimating hydraulic parameters in a 3D sand tank using silica encapsulated magnetic DNA particles. *Adv. Water. Resour.* 179. <https://doi.org/10.1016/j.advwatres.2023.104507>.
- Chakraborty, S., Panigrahi, P.K., 2020. Stability of nanofluid: a review. *Appl. Therm. Eng.* 174. <https://doi.org/10.1016/j.applthermaleng.2020.115259>.
- Christensen, H.K., 1988. Non-DLVO forces between surfaces - solvation, hydration and capillary effects. *J. Dispers. Sci. Technol.* 9. <https://doi.org/10.1080/01932698808943983>.
- Derjaguin, B., Landau, L., 1941. Theory on the stability of strongly charged lyophobic sols and of the adhesion of strongly charged particles in solutions of electrolytes. *Acta Physico Chemica URSS* 14, 30. [https://doi.org/10.1016/0079-6816\(93\)90013-L](https://doi.org/10.1016/0079-6816(93)90013-L).
- Elimelech, M., Gregory, J., Jia, X., Williams, R.A., 1995. *Particle Deposition & Aggregation - Measurement, Modeling and Simulation*. Butterworth-Heinemann.
- Elimelech, M., O'Melia, C.R., 1990. Kinetics of deposition of colloidal particles in porous media. *Environ. Sci. Technol.* 24. <https://doi.org/10.1021/es00080a012>.
- Fan, K.-C., Gao, P.-J., Chen, B.-H., Han, Y.-L., Cheng, C.-L., 2024. Development and application of a geothermal bio-tracer resistant to extreme environments. *Geothermics* 119. <https://doi.org/10.1016/j.geothermics.2024.102982>.
- French, R.H., Winey, K.I., Yang, M.K., Qiu, W., 2007. Optical properties and van der Waals-London dispersion interactions of polystyrene determined by vacuum ultraviolet spectroscopy and spectroscopic ellipsometry. *Aust. J. Chem.* 60. <https://doi.org/10.1071/CH06222>.
- Gazem, A., Patel, H., Sreenivasan, H., Sahu, C., Krishna, S., 2024. Combined effect of silica nanoparticles and binary surfactants in enhancing oil recovery: an experimental investigation. *Colloids Surf. A: Physicochem. Eng. Aspects* 702. <https://doi.org/10.1016/j.colsurfa.2024.134980>.
- Ghosh, S.K., Alargova, R.G., Deguchi, S., Tsujii, K., 2006. Dispersion stability of colloids in sub- and supercritical water. *J. Phys. Chem. B*. <https://doi.org/10.1021/jp0656328>.
- Gregory, J., 1981. Approximate expressions for retarded van der Waals interaction. *J. Colloid. Interface Sci.* 83. [https://doi.org/10.1016/0021-9797\(81\)90018-7](https://doi.org/10.1016/0021-9797(81)90018-7).
- Hartmann, R., Kinnunen, P., Ilikainen, M., 2018. Cellulose-mineral interactions based on the DLVO theory and their correlation with flotability. *Miner. Eng.* 122, 9. <https://doi.org/10.1016/j.mineng.2018.03.023>.
- Healy, T.W., La Mer, V.K., 1964. The energetics of flocculation and redispersion by polymers. *J. Colloid. Interface Sci.* 19. [https://doi.org/10.1016/0095-8522\(64\)90034-0](https://doi.org/10.1016/0095-8522(64)90034-0).
- Higgo, J.J.W., Williams, G.M., Harrison, I., Warwick, P., Gardiner, M.P., Longworth, G., 1993. Colloid transport in a glacial sand aquifer: laboratory and field studies. *Colloids Surf. A: Physicochem. Eng. Aspects* 73, 22. [https://doi.org/10.1016/0927-7757\(93\)80015-7](https://doi.org/10.1016/0927-7757(93)80015-7).
- Hogg, R., Healy, T.W., Fuerstka, D.W., 1966. Mutual coagulation of colloidal dispersions. *Trans. Faraday Soc.* 62. <https://doi.org/10.1039/TF9666201638>.
- Hull, M., Kitchener, J.A., 1969. Interaction of spherical colloidal particles with planar surfaces. *Trans. Faraday Soc.* 65. <https://doi.org/10.1039/TF9696503093>.
- Ishido, T., Mizutani, H., 1981. Experimental and theoretical basis of electrokinetic phenomena in rock-water systems and its applications to geophysics. *J. Geophys. Res.* 86. <https://doi.org/10.1029/jb086ib03p01763>.
- Izrael-Zivković, L.T., Živković, L., Jokić, B.M., Savić, A.V., Karadžić, I.M., 2015. Adsorption of *Candida rugosa* lipase onto alumina: effect of surface charge. *J. Serb. Chem. Soc.* 80. <https://doi.org/10.2298/JSC150222035I>.
- Jia, F., Li, H., Liu, Z., Li, Y., Ma, X., Zhang, G., Zhang, Q., 2024. Study on the adsorption mechanism of fluorescent nano-tracer in sandstone core. *J. Environ. Chem. Eng.* 12. <https://doi.org/10.1016/j.jece.2024.113560>.
- Jiang, K., Pinchuk, P., 2016. Temperature and size-dependent Hamaker constants for metal nanoparticles. *Nanotechnology* 27. <https://doi.org/10.1088/0957-4484/27/34/345710>.
- Jódar-Reyes, A.B., Martín-Rodríguez, A., Ortega-Vinuesa, J.L., 2006. Effect of the ionic surfactant concentration on the stabilization/destabilization of polystyrene colloidal particles. *J. Colloid. Interface Sci.* 298. <https://doi.org/10.1016/j.jcis.2005.12.035>.
- Kittilä, A., Jalali, M.R., Evans, K.F., Willmann, M., Saar, M.O., Kong, X.-Z., 2019. Field comparison of DNA-labeled nanoparticle and solute tracer transport in a fracture crystalline rock. *Water. Resour. Res.* 55 (8), 19. <https://doi.org/10.1029/2019WR025021>.
- Klaine, S.J., Alvarez, P.J.J., Batley, G.E., Fernandes, T.F., Handy, R.D., Lyon, D.Y., Mahendra, S., McLaughlin, M.J., Lead, J.R., 2009. Nanomaterials in the environment: behavior, fate, bioavailability and effects. *Environ. Toxicol. Chem.* 27. <https://doi.org/10.1897/08-090.1>.
- Kong, X.-Z., Deuber, C.A., Kittilä, A., Somogyvári, M., Mikutis, G., Bayer, P., Stark, W.J., Saar, M.O., 2018. Tomographic reservoir imaging with DNA-labeled silica nanotracers: the first field validation. *Environ. Sci. Technol.* 52 (23), 9. <https://doi.org/10.1021/acs.est.8b04367>.
- Lefèvre, G., & Jolivet, A. (2009). Calculation of Hamaker constants applied to the deposition of metallic oxide particles at high temperatures. *Proceedings of International Conference on Heat Exchanger Fouling and Cleaning VIII*.
- Li, Y.V., Cathles, L.M., Archer, L.A., 2014. Nanoparticle tracers in calcium carbonate porous media. *J. Nanopart. Res.* 16. <https://doi.org/10.1007/s11051-014-2541-9>.
- Liu, G., Zhong, H., Ahmad, Z., Yang, X., Huo, L., 2019. Transport of engineered nanoparticles in porous media and its enhancement for remediation of contaminated groundwater. *Crit. Rev. Environ. Sci. Technol.* 50. <https://doi.org/10.1080/10643389.2019.1694823>.
- Marshall, J.K., Kitchener, J.A., 1966. The deposition of colloidal particles on smooth solids. *J. Colloid. Interface Sci.* 22. [https://doi.org/10.1016/0021-9797\(66\)90014-2](https://doi.org/10.1016/0021-9797(66)90014-2).
- Mikutis, G., Deuber, C.A., Schmid, L., Kittilä, A., Lobsiger, N., Puddu, M., Asgeirsson, D. O., Grass, R.N., Saar, M.O., Stark, W.J., 2018. Silica-encapsulated DNA-based tracers for aquifer characterization. *Environ. Sci. Technol.* 52 (21), 11. <https://doi.org/10.1021/acs.est.8b03285>.
- Muneer, R., Hashmet, M.R., Pourafshary, P., 2022. DLVO modeling to predict critical salt concentration to initiate fines migration pre- and post-nanofluid treatment in sandstones. *SPE J.* 27. <https://doi.org/10.2118/209588-PA>.
- Muneer, R., Rehan Hashmet, M., Pourafshary, P., 2020. Fine migration control in sandstones: surface force analysis and application of DLVO theory. *ACS Omega* 5 (49), 16. <https://doi.org/10.1021/acsomega.0c03943>.
- Napper, D.H., Netschey, A., 1971. Studies of the steric stabilization of colloidal particles. *J. Colloid. Interface Sci.* 37. [https://doi.org/10.1016/0021-9797\(71\)90330-4](https://doi.org/10.1016/0021-9797(71)90330-4).
- Ninham, B.W., 1999. On progress in forces since the DLVO theory. *Adv. Colloid. Interface Sci.* 83. [https://doi.org/10.1016/S0001-8686\(99\)00008-1](https://doi.org/10.1016/S0001-8686(99)00008-1).
- Paunescu, D., Puddu, M., Soellner, J.O., Stoessel, P.R., Grass, R.N., 2013. Reversible DNA encapsulation in silica to produce ROS-resistant and heat-resistant synthetic DNA 'fossils'. *Nat. Prot.* 8. <https://doi.org/10.1038/nprot.2013.154>.
- Pinchuk, P., Jiang, K., 2015. Size-dependent Hamaker constant for silver and gold nanoparticles. *Phys. Chem. Interfaces Nanomater.* XIV.
- Qiao, Z.-A., Zhang, L., Guo, M., Liu, Y., Huo, Q., 2009. Synthesis of mesoporous silica nanoparticles via controlled hydrolysis and condensation of silicon alkoxide. *Chem. Mater.* 21. <https://doi.org/10.1021/cm901335k>.
- Radilla, G., Sausse, J., Sanjuan, B., Fourar, M., 2012. Interpreting tracer tests in the enhanced geothermal system (EGS) of Soultz-sous-Forêts using the equivalent stratified medium approach. *Geothermics* 44. <https://doi.org/10.1016/j.geothermics.2012.07.001>.
- Ruckenstein, E., Prieve, D.C., 1976. Adsorption and desorption of particles and their chromatographic separation. *AIChE J.* <https://doi.org/10.1002/aic.690220209>.
- Rudolph, B., 2021. *Reporting Nanoparticle Tracers - Entwicklung von Thermoresponsiven Tracern für geothermische Anwendungen*. Karlsruhe Institute of Technology. J.
- Rudolph, B., Berson, J., Held, S., Nitschke, F., Wenzel, F., Kohl, T., Schimmel, T., 2020. Development of thermo-reporting nanoparticles for accurate sensing of geothermal reservoir conditions. *Sci. Rep.* 10 (1). <https://doi.org/10.1038/s41598-020-68122-y>.
- Ryan, J.N., Elimelech, M., 1996. Colloid mobilization and transport in groundwater. *Colloids Surf. A: Physicochem. Eng. Aspects* 107, 56. [https://doi.org/10.1016/0927-7757\(95\)03384-X](https://doi.org/10.1016/0927-7757(95)03384-X).
- Sanjuan, B., Pinault, J.-L., Rose, P., Gérard, A., Brach, M., Braibant, G., Crouzet, C., Foucher, J.-C., Gautier, A., Touzelet, S., 2006. Tracer testing of the geothermal heat exchanger at Soultz-sous-Forêts (France) between 2000 and 2005. *Geothermics* 35 (5–6), 32. <https://doi.org/10.1016/j.geothermics.2006.09.007>.
- Sanjuan, B.M., R., Innocent, C., Dezayes, C., Scheiber, J., Brach, M., 2016. Major geochemical characteristics of geothermal brines from the Upper Rhine Graben granitic basement with constraints on temperature and circulation. *Chem. Geol.* 428. <https://doi.org/10.1016/j.chemgeo.2016.02.021>.
- Silencioux, F., Bouchoucha, M., Mercier, O., Turgeon, S., Chevallier, P., Kleitz, F., Fortin, M.-A., 2015. Mesoporous silica nanoparticles under sintering conditions: a quantitative study. *Langmuir* 31. <https://doi.org/10.1021/acs.langmuir.5b02961>.
- Spitzmüller, L., Berson, J., Nitschke, F., Kohl, T., Schimmel, T., 2024a. Titania-mediated stabilization of fluorescent dye encapsulation in mesoporous silica nanoparticles. *Nanoscale Adv.* 6. <https://doi.org/10.1039/D4NA00242C>.
- Spitzmüller, L., Berson, J., Schimmel, T., Kohl, T., Nitschke, F., 2024b. Temperature stability and enhanced transport properties by surface modifications of silica nanoparticle tracers for geo-reservoir exploration. *Sci. Rep.* 14. <https://doi.org/10.1038/s41598-024-70132-z>.
- Spitzmüller, L., Nitschke, F., Maercks, A., Berson, J., Rudolph, B., Schimmel, T., & Kohl, T. (2023a). Nanoparticle-based tracing techniques in geothermal reservoirs: advances, challenges and prospects. 4th Workshop on Geothermal Reservoir Engineering, Stanford University, Stanford, California.
- Spitzmüller, L., Nitschke, F., Rudolph, B., Berson, J., Schimmel, T., Kohl, T., 2023b. Dissolution control and stability improvement of silica nanoparticles in aqueous media. *J. Nanopart. Res.* 25 (3). <https://doi.org/10.1007/s11051-023-05688-4>.

- Tang, Y., Zhang, F., Boogard, T., Chassagne, C., Ali, Z., Bandyopadhyay, S., Foppen, J.W., 2023. Settling of superparamagnetic silica encapsulated DNA microparticles in water. *Hydrol. Process.* 37. <https://doi.org/10.1002/hyp.14801>.
- Tian, Y., Gao, B., Silvera-Batista, C., Ziegler, K.J., 2010. Transport of engineered nanoparticles in saturated porous media. *J. Nanopart. Res.* 12. <https://doi.org/10.1007/s11051-010-9912-7>.
- Tosha, T., Matsushima, N., Ishido, T., 2003. Zeta potential measured for an intact granite sample at temperatures to 200 °C. *Geophys. Res. Lett.* 30. <https://doi.org/10.1029/2002GL016608>.
- Tran, E., Richmond, G.L., 2021. Interfacial steric and molecular bonding effects contributing to the stability of neutrally charged nanoemulsions. *Langmuir* 37. <https://doi.org/10.1021/acs.langmuir.1c02020>.
- Tufenkji, N., Elimelech, M., 2004. Correlation equation for predicting single-collector efficiency in physicochemical filtration in saturated porous media. *Environ. Sci. Technol.* 38 (2). <https://doi.org/10.1021/es034049r>.
- Valmacco, V., Elzbieciak-Wodka, M., Besnard, C., Maroni, P., Trefalt, G., Borkovec, M., 2016. Dispersion forces acting between silica particles across water: influence of nanoscale roughness. *Nanoscale Horiz.* 4. <https://doi.org/10.1039/C6NH00070C>.
- van Oss, C.J., 2008. The extended DLVO theory. *Interface Sci. Technol.* 16. [https://doi.org/10.1016/S1573-4285\(08\)00203-2](https://doi.org/10.1016/S1573-4285(08)00203-2).
- Verwey, E.J.W., Overbeek, J.T.G., 1948. *Theory of the Stability of Lyophobic Colloids; the Interaction of Sol Particles Having an Electric Double Layer*. Elsevier.
- Vincent, B., Edwards, J., Emmett, S., Jones, A., 1986. Depletion flocculation in dispersions of sterically-stabilised particles ("soft spheres"). *Colloids Surf.* 18. [https://doi.org/10.1016/0166-6622\(86\)80317-1](https://doi.org/10.1016/0166-6622(86)80317-1).
- Walker, E., Glover, P.W.J., 2018. Measurements of the relationship between microstructure, pH, and the streaming and zeta potential of sandstones. *Transp. Porous Mater.* 121. <https://doi.org/10.1007/s11242-017-0954-5>.
- Wang, Y., Wang, L., Hampton, M.A., Nguyen, A.V., 2013. Atomic force microscopy study of forces between a silica sphere and an oxidized silicon wafer in aqueous solutions of NaCl, KCl, and CsCl at concentrations up to saturation. *J. Phys. Chem. C* 117. <https://doi.org/10.1021/jp3092495>.
- Worthen, A.J., Tran, V., Cornell, K.A., Truskett, T.M., Johnston, K.P., 2016. Steric stabilization of nanoparticles with grafted low molecular weight ligands in highly concentrated brines including divalent ions. *RSC Soft Matter* 12, 15. <https://doi.org/10.1039/C5SM02787J>.
- Xie, Q., Saeedi, A., Pooryousefy, E., Liu, Y., 2016. Extended DLVO-based estimates of surface force in low salinity water flooding. *J. Mol. Liq.* 221. <https://doi.org/10.1016/j.molliq.2016.06.004>.
- Xu, S., Gao, B., Saiers, J.E., 2006. Straining of colloidal particles in saturated porous media. *AGU Water Resour. Res.* 42. <https://doi.org/10.1029/2006WR004948>.
- Yan, Z., Huang, X., Yang, C., 2014. Deposition of colloidal particles in a microchannel at elevated temperatures. *Microfluid. Nanofluid.* 18. <https://doi.org/10.1007/s10404-014-1448-1>.
- Zareei, M., Yoozbashizadeh, H., Madaah Hosseini, H.R., 2018. Investigating the effects of pH, surfactant and ionic strength on the stability of alumina/water nanofluids using DLVO theory. *J. Therm. Anal. Calorim.* 135. <https://doi.org/10.1007/s10973-018-7620-1>.
- Zaucha, M., Adamczyk, Z., Barbasz, J., 2011. Zeta potential of particles bilayers on mica: a streaming potential study. *J. Colloid. Interface Sci.* 360. <https://doi.org/10.1016/j.jcis.2011.02.025>.
- Zhulina, E.B., Borisov, O.V., Priamitsyn, V.A., 1990. Theory of steric stabilization of colloid dispersions by grafted polymer. *J. Colloid. Interface Sci.* 137. [https://doi.org/10.1016/0021-9797\(90\)90423-L](https://doi.org/10.1016/0021-9797(90)90423-L).